Electronic Supplementary Material (ESI) for Journal of Materials Chemistry

Highly entangled $K_{0.5}V_2O_5$ superlong nanobelts membrane for flexible nonvolatile memory device

Kun Xu,[a‡] Shuanglin Hu,[b‡] Changzheng Wu,[a] Chenwen Lin,[a] Xiuli Lu,[a] Lele Peng,[a] Jinlong Yang,[a] Yi Xie[a]**

Supporting information

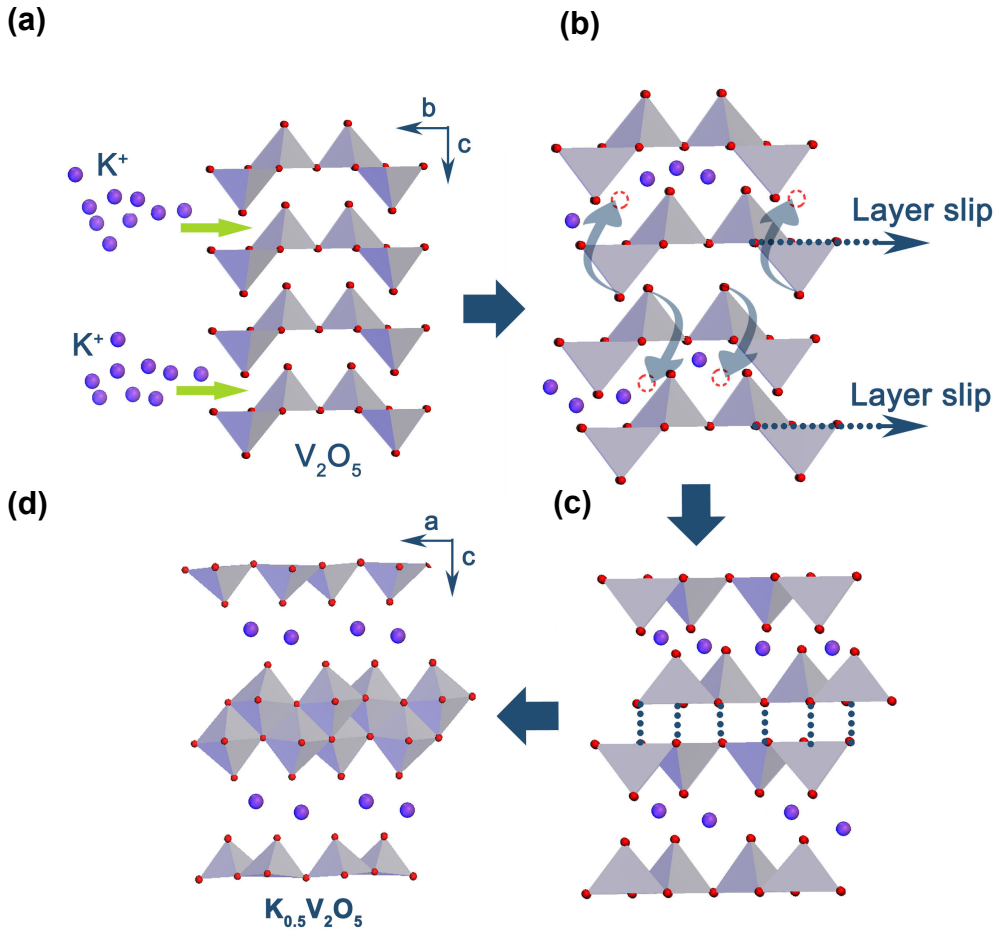

Figure S1. The structural evolution from V_2O_5 to $K_{0.5}V_2O_5$. (a) Insertion and diffusion of potassium ions leads to their entry into the layers, the distortion at the edge of the lattice enable the insertion process occur more easily every two layers. (b) Subsequently, triggered by the K+ insertion, the layer slips, and the VO_5 square pyramid would turn backward by following by the classic motion style of VO_5. (c) Driven by the lower thermodynamically energy, the vanadium atoms would rearrange in the lattices and re-bonding to form the stable V-O framework configurations. (d) The $K_{0.5}V_2O_5$ layered structure finally formed after the structural evolution process (K^+ ions occupy half of the available sites).

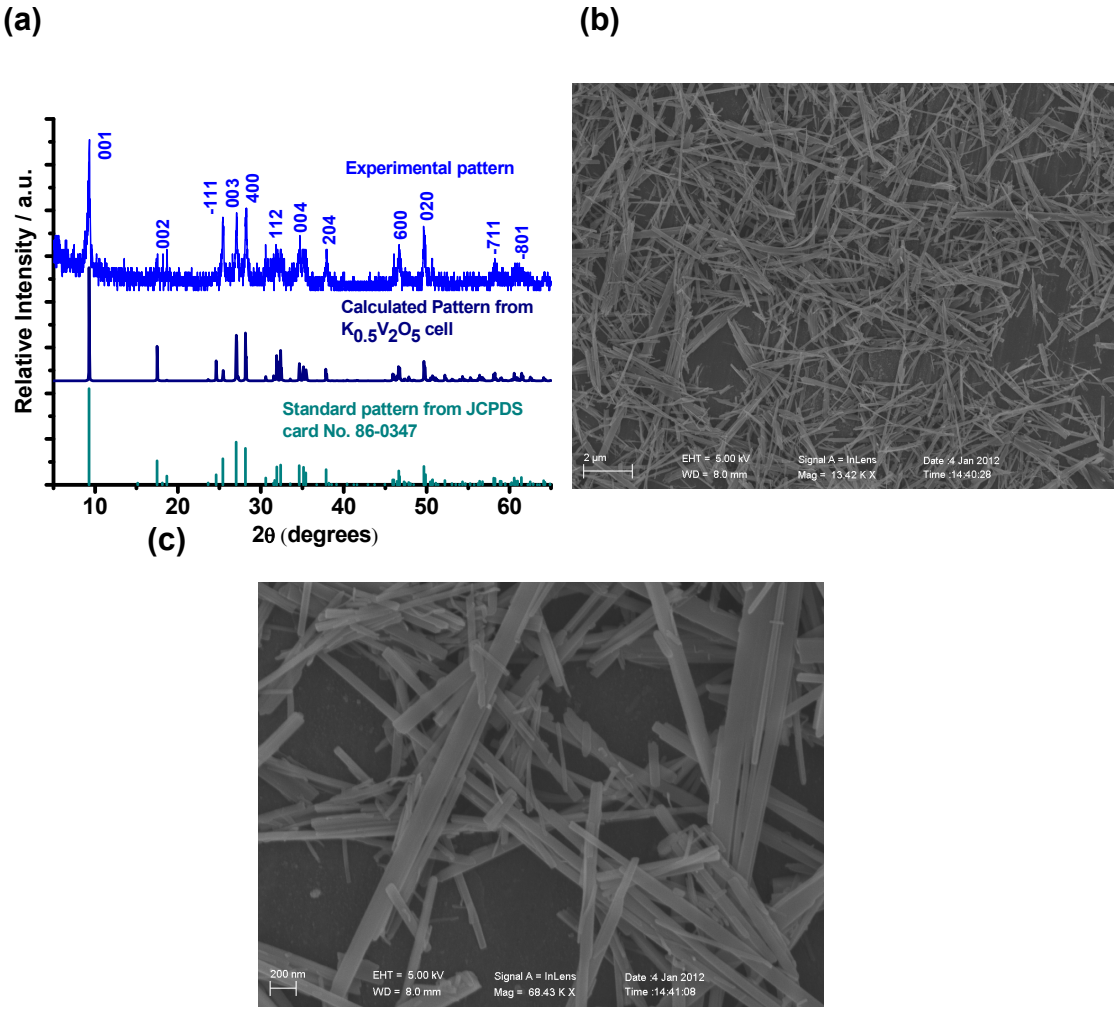

Figure S2. (a)Experimental (top)，simulated (middle)，and standard (bottom) XRD pattern of the $K_{0.5}V_2O_5$ nanobelts. (b, c) Low- and high-magnification FESEM images of the as-prepared $K_{0.5}V_2O_5$ nanobelts.

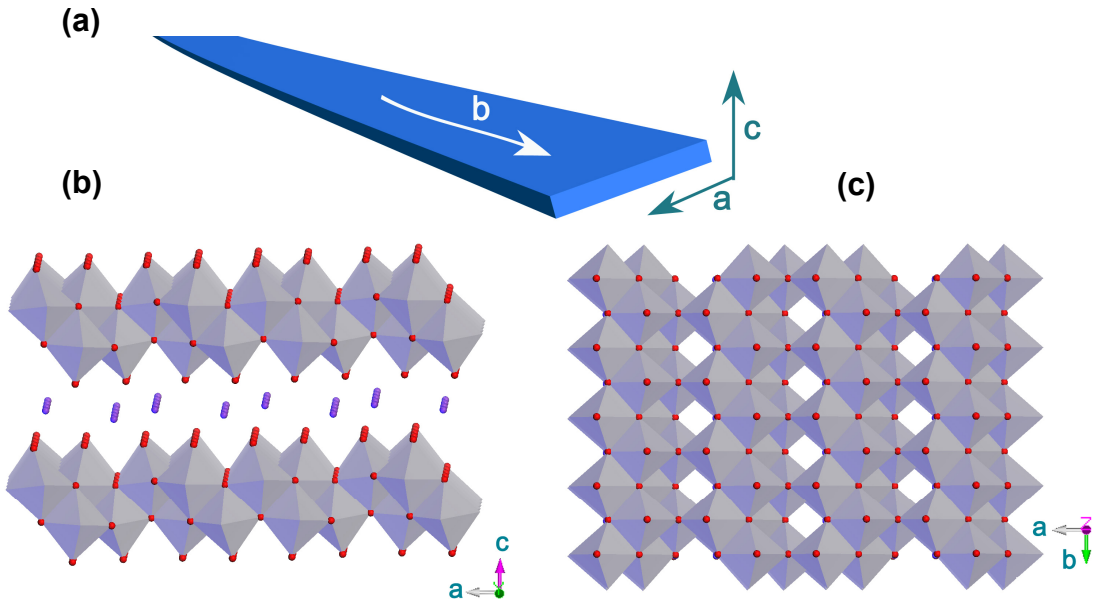

Figure S3. (a) Schematic illustration of the nanobelt growth direction. (b-c) polyhedral-style supercell model of the $K_{0.5}V_2O_5$ projected along b axis (b) and along c axis (c).

The anisotropy of the potassium vanadium oxide nanobelt is stemmed from the lattice packing characteristics of the crystal. As shown in Figure S3, Generally, the δ-$K_{0.5}V_2O_5$ structure has a layered framework with the space group of C2/m, indicating the difference between the atomic crystal lattice along the a/b-axis and that along the c-axis. Therefore, the crystal growth along c-axis would be suppressed due to the weak interlayer interaction force between each two V_2O_5 layers. This suppression leads to the crystal expansion within the a-b plane. Moreover, as shown in Figure S3 (c), a–b plane of the δ-$K_{0.5}V_2O_5$ structure exhibits tunnels with square cross sections, in which the b axis has tightly linked VO_6 octahedrons forming close-stacked vanadium chains. However, tunnel structure can be clearly seen along a-axis, leading to a lower stacking-density. In this regard, the crystalline preference along b-axis in the growth process of δ-$K_{0.5}V_2O_5$ nanobelt is understandable.

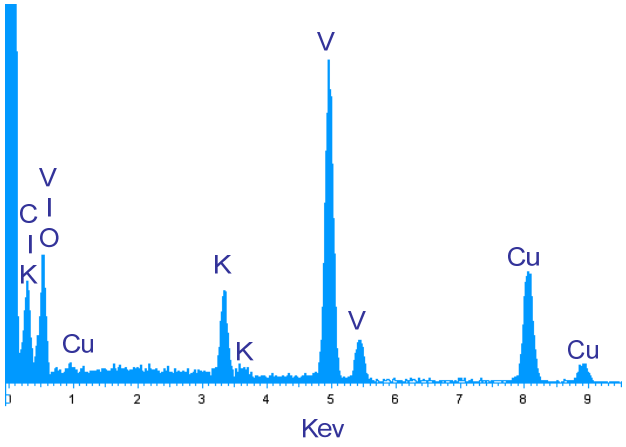

Figure S4. EDX spectra of the synthetic $K_{0.5}V_2O_5$ nanobelt.

S5. SAED pattern analysis

The angle values between the lattice planes that appeared in the SAED patterns provide the direct evidence for bronze δ-$K_{0.5}V_2O_5$ and the growth direction of the one-dimensiaonal nanobelt. The experimental angle value was achieved by directly determining the corresponding angle between the two lines, where the lines were formed by the linkage of each of two points, which represents the concerned two lattice planes, with the zone-axis point in the same SAED pattern, respectively. Theoretical angle value was obtained by the crystallographic parameters calculation based on the monoclinic bronze $K_{0.5}V_2O_5$. The relevant formula was shown as follows:

$$\cos\varphi = \frac{\frac{h_1h_2}{a^2\sin^2\beta} + \frac{k_1k_2}{b^2} + \frac{l_1l_2}{c^2\sin^2\beta} - \frac{(h_1l_2 + l_1h_2)\cos\beta}{ac\sin^2\beta}}{\left[\left(\frac{h_1^2}{a^2\sin^2\beta} + \frac{k_1^2}{b^2} + \frac{l_1^2}{c^2\sin^2\beta} - \frac{2h_1l_1\cos\beta}{ac\sin^2\beta}\right)\cdot\left(\frac{h_2^2}{a^2\sin^2\beta} + \frac{k_2^2}{b^2} + \frac{l_2^2}{c^2\sin^2\beta} - \frac{2h_2l_2\cos\beta}{ac\sin^2\beta}\right)\right]^{1/2}}$$

Where h, k, l were the miller indices of the crystallographic planes, β is the characteristic angle for the monoclinic structure, and a, b, c were the crystal parameters in monoclinic bronze $K_{0.5}V_2O_5$.

All the experimental and calculated results were summarized in Table 1, where the experimental angle values agree well with the corresponding calculation ones, giving the solid evidence that the as-obtained vanadium dioxides was monoclinic bronze $K_{0.5}V_2O_5$ with JCPDS Card No. 86-0347. Also, the combination analysis of the SAED pattern and the growth nanobelts clearly reveals that the growth direction of the nanobelts is along [020], i.e. *b*-axis.

Table 1. The summary information of the experimental angle values and the theoretical angle values for the as-obtained monoclinic bronze $K_{0.5}V_2O_5$ ultralong nanobelts.

Lattice Plane		Theoretical Angle Value	Experimental Angle Value
(200)	(110)	72.56	72.8
	(020)	90.00	90.0
(020)	(110)	17.43	17.3

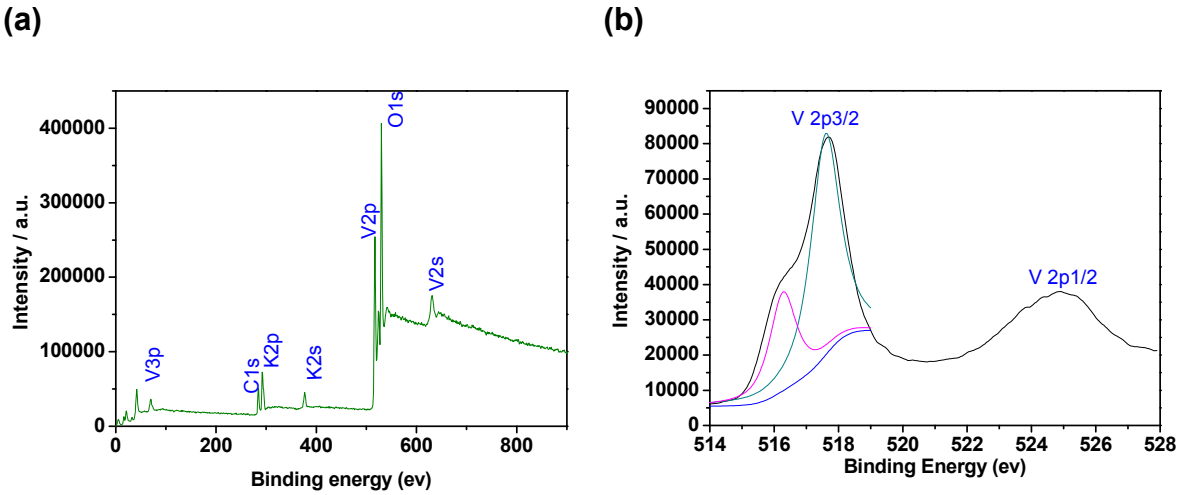

Figure S6. (a) XPS spectra of potassium vanadium oxide nanobelts. (b) XPS spectra of V 2p peak.

The XPS was used to further investigation the composition of the our samples as well as the valence state of vanadium ions. In the XPS spectra (Figure S6a), it is found that our sample only consist of potassium, vanadium, oxide and no iodine ion and chloridion existed which was also proved that our samples were high quality. It should pointed out that the binding energies in the XPS spectra were corrected by referencing the C1s to 280.6eV. The two peaks (Figure S6b) centered at 517.7eV and 524.8eV correspond to the V2p3/2 and V2p1/2 of V^{5+}, respectively.[1] Careful analysis of the V high resolution spectra, the existence of overlapping peak located at 516.3eV with less intensity was found illustrates that a small amount of V^{4+} in our samples.[2]

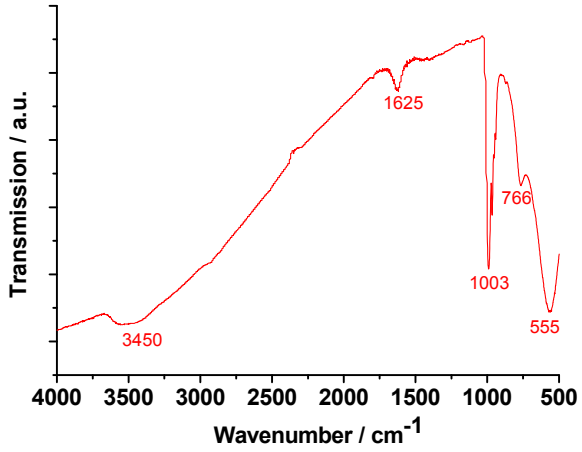

Figure S7. IR spectra of potassium vanadium oxide nanobelts.

Figure S7 shows the IR spectra of potassium vanadium oxide nanobelt. The absorption bands at 3450 and 1625cm^{-1} are the stretching of O-H and flexural vibrations of the O-H ascribe to the existence of the free water in the samples. The signals at 1003cm^{-1} correspond to the V=O stretching vibration, respectively.[3] The red shift of the V=O stretching vibration due to the part of V^{5+} were reduced to V^{4+}.[4] The absorption bands locating at 766 and 555$cm^{-1}$are attributed to the in-plane and out-of-plane V-O-V vibrations.[3]

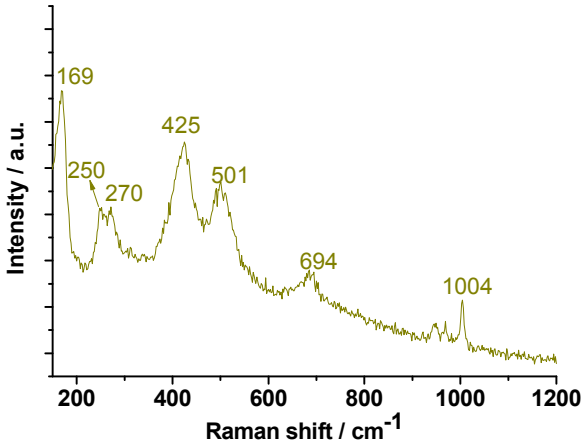

Figure S8. Raman scattering spectrum of potassium vanadium oxide nanobelts.

The low wavenumber peaks locating at 169cm^{-1} due to the external modes of the derivative of the V_2O_5 units.[5] The bands at 270 and 425cm^{-1} are assigned to the bending vibration of the V=O bonds.[5] The peaks at 501 and 694cm^{-1} are attributed to V-O stretching modes.[5-6] The peak of 1004cm^{-1}, a spectral fingerprint of the δ-phase, corresponding to the stretching modes of the V=O moiety.[5]

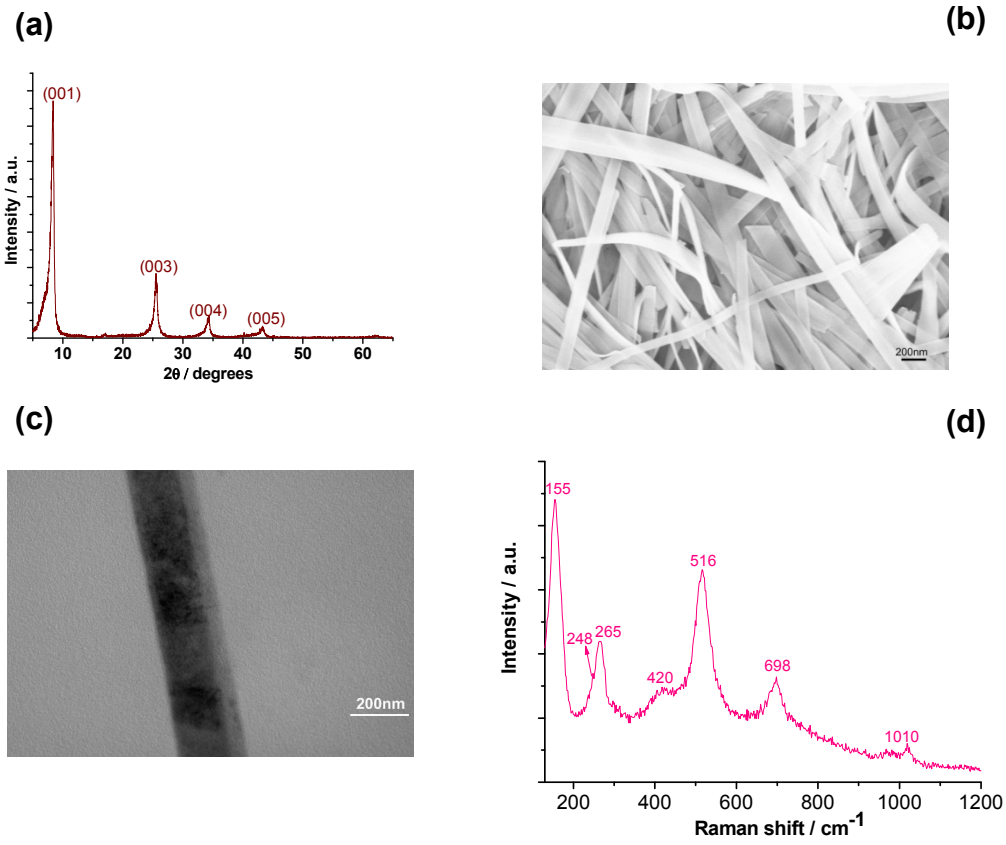

Figure S9. (a) XRD pattern of $Li_xV_2O_5$. (b) FESEM images of the as-prepared $Li_xV_2O_5$ nanobelts. (c) TEM images of the as-prepared $Li_xV_2O_5$ nanobelts. (d) Raman scattering spectrum of $Li_xV_2O_5$ nanobelts.

Preparation of the $Li_xV_2O_5$ nanobelts was similar to the preparation of the $K_{0.5}V_2O_5$ nanobelts. The XRD pattern of the as-synthesized lithium vanadium oxide nanobelts, as shown in Figure S9a, which cannot be indexed to any XRD patterns presented in the Joint Committee on Powder Diffraction Standards (JCPDS) cards but very similar to the vanadium oxide xerogels by a previous report.[7] The FESEM and TEM images of the synthetic $Li_xV_2O_5$ (Figure S9b and c) clearly demonstrate that the samples owns nanobelt performance. The raman scattering spectrum of $Li_xV_2O_5$ nanobelts was shown in Figure S9d, the peak of 1010cm^{-1} which was a spectral fingerprint of

the δ-phase correspond to the stretching modes of the V=O moiety was detected direct illustrate that our $Li_xV_2O_5$ nanobelts belong to δ-$M_xV_2O_5$ bronze .[5]

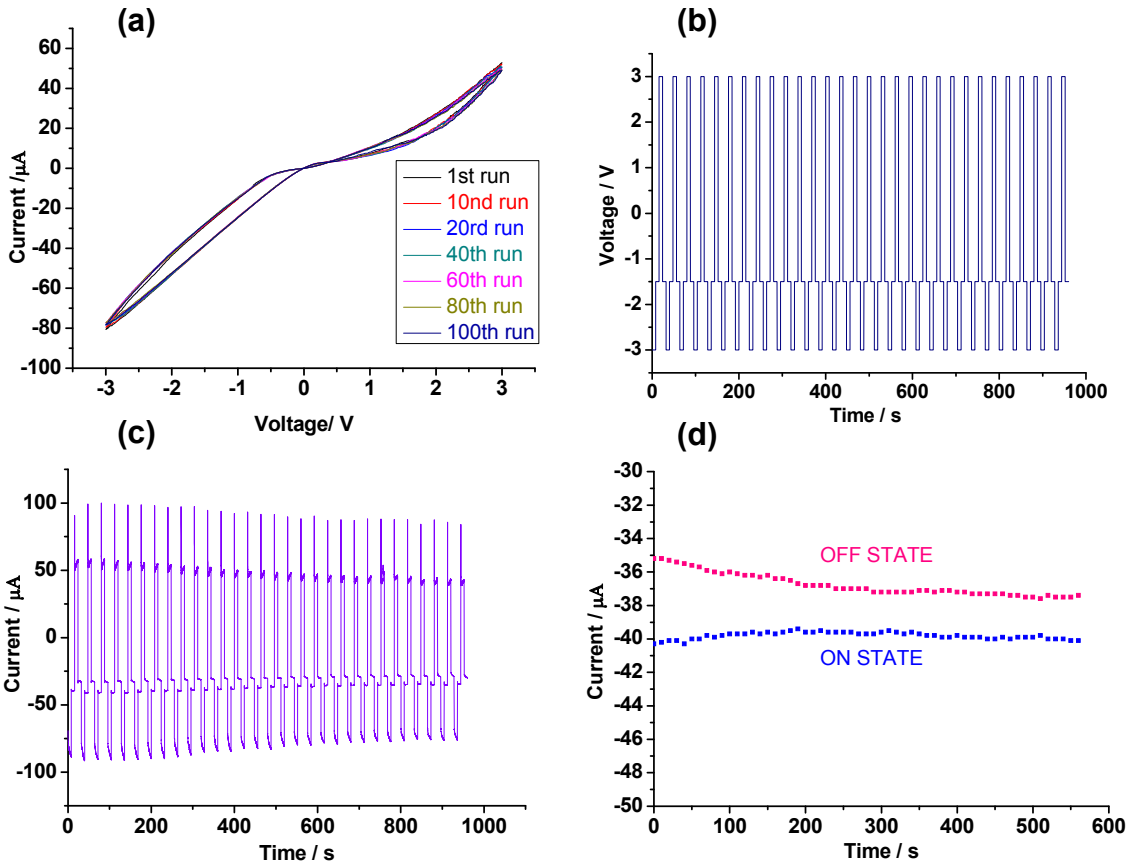

Figure S10. (a) I-V characteristic of the memristor based on $Li_xV_2O_5$ nanobelts measured with repeated voltage scan 0.1V/s. (b) Input of the WRER cycles of the memristor based $Li_xV_2O_5$ nanobelts, for rewritable data storage application. Voltage: W, -3.0; R, -1.5; E, +3.0; and R, -1.5V. (c) Output of the WRER cycles. (d) Retention times of the ON and OFF states of the memristor based $Li_xV_2O_5$ nanobelts, probed with currents under -1.5V. The ON and OFF states were induced by -3.0V (W) and 3.0V (E), respectively.

We should noted that the condition of the I-V characteristic of the memristor based on $Li_xV_2O_5$ nanobelts was same to the I-V characteristic of the memristor based on $K_xV_2O_5$ superlong naobelts membrane. The memristor based on $Li_xV_2O_5$ nanobelts also need a forming process. After a forming process, the I-V curves of the memristor based on $Li_xV_2O_5$ nanobelts take on stable, reversible and nonlinear hysteresis behavior in nature, too. The stable current hysteresis could be well repeated during the continuous voltage sweeping over 100 times (Figure S10a). A series of "write-read-erase-read" (WRER) cycles (Figure S10b) were also tested to further check up the stability of our device based on $Li_xV_2O_5$. Reading voltage all along at -1.5V for 8s and the write and erase programmes was induced by a pulse voltage at -3.0V and 3.0V also for 8s at each cycle. The results of the WRER cycles of the memristor based on $Li_xV_2O_5$ nanobelts clearly shows that it was less stable compare with the memristor based on $K_{0.5}V_2O_5$ superlong naobelts membrane (Figure S10c and Figure 5c). The ON and OFF states were induced by pulse voltage at -3.0 and 3.0V, respectively. As shown in Figure S10d, the retention times of the ON and OFF state of the memristor based on $Li_xV_2O_5$ nanobelts over 600s were detected certify that it also could be used as nonvolatile memory device.[8]

References

1. G. A. Sawatzky and D. Post, *Phys. Rev. B*, 1979, **20**, 1546-1555.
2. J. Mendialdua, R. Casanova and Y. Barbaux, *J. Electron Spectroc. Relat. Phenom.*, 1995, **71**, 249-261.
3. C. V. Subba Reddy, S.-i. Mho, R. R. Kalluru and Q. L. Williams, *J. Power Sources*, 2008, **179**, 854-857.
4. Y. Chen, G. Yang, Z. Zhang, X. Yang, W. Hou and J.-J. Zhu, *Nanoscale*, 2010, **2**, 2131-2138.
5. R. Baddour Hadjean, J. P. Pereira Ramos, C. Navone and M. Smirnov, *Chem. Mater.*, 2008, **20**, 1916-1923.
6. Y. Wei, C. W. Ryu and K. B. Kim, *J. Power Sources*, 2007, **165**, 386-392.
7. V. Petkov, P. N. Trikalitis, E. S. Bozin, S. J. L. Billinge, T. Vogt and M. G. Kanatzidis, *J. Am. Chem. Soc.*, 2002, **124**, 10157-10162.
8. J. Lee, H. Chang, S. Kim, G. S. Bang and H. Lee, *Angew. Chem. In. Ed.*, 2009, **48**, 8501-8504.